From the Department of Clinical Neuroscience and
the Center for Hearing and Communication Research,
Karolinska Institutet, Stockholm, Sweden

IMAGING THE ORGAN OF CORTI IN VITRO AND IN VIVO

Igor Tomo

Karolinska Institutet

Stockholm 2009

Published by Karolinska Institutet. Printed by Larserics, Sundbyberg, Sweden

ISBN 978-91-7409-463-3

To my parents.

Nothing worth having comes easy

ABSTRACT

Recent developments in imaging techniques, namely confocal laser scanning microscopy, offer new tools in exploration of the structure and function of the inner ear. The optical sectioning property of the confocal microscope enables investigation of living cells deeper within a labeled intact tissue. This key feature has been embraced in all three our projects, using both in-vitro and in-vivo approaches.

In the first study, we have developed an in-vivo model for confocal imaging of the cochlear structure in living guinea pigs. Temporal bones have been used previously for visualization in the unfixed cochlea. There is however an inevitable time limitation in all in-vitro preparations, caused by interruption of blood and nerve supply and gradual disappearance of endocochlear potential, which occurs just few hours after temporal bone dissection. Thus in-vitro models may not faithfully reflect the whole complexity of the inquired system. In-vivo preparation is deemed to be superior to in-vitro one, due to its closeness to physiological conditions. Obviously, this approach is much more demanding, especially when depicting a delicate, bone encapsulated and fluid filled structure of the cochlea in sub-optimal imaging conditions. Apart from morphology we have also investigated pathological changes induced by acoustic overstimulation. Shortening and swelling of the hair cells which was observed, coincides with results of similar experiments performed on isolated temporal bones. For the first time, we have presented detailed confocal images acquired from the living inner ear with its blood and nerve supply still preserved.

Confocal laser scanning microscopy has one substantial limitation in a relatively long acquisition time. Due to the inherent point-to-point scanning mode of the microscope, it takes up to 1 second to acquire a single standard size confocal image. This is too slow to capture a swift, oscillatory motion of the organ of Corti during sound stimulation. However, a pixel dwell time of the microscope is much shorter - in the range of microseconds. This fact was utilized in the second project, with the aim to develop a confocal imaging method to visualize and measure the rapid motion patterns of stereocilia during the sound stimulation. Using a temporal bone preparation of the guinea pig cochlea, two dimensional, high-resolution images were acquired from structures vibrating at frequencies up to several hundred Hertz. Results here show that under passive conditions, the outer hair cell stereocilia deflection is larger then in the inner hair cells. Phase relations were consistent with an idea that stimulation of inner hair cells occurs through the surrounding fluid drag. The small deflection amplitudes that we measured presume active amplification present not only in the outer hair cells but also in the inner ones.

Our third project stemmed from the previously described technique, which was further improved by computing the Fourier series coefficients for each acquired pixel along the time dimension. Technical improvements resulted in faster acquisition times while using larger image format (512x512pixels) and increased sound stimulation frequency interval up to 500Hz. Data measured at different sound stimulation levels from both outer and inner hair cells at the identical regions of cochlea show, that the reticular lamina does not vibrate as a stiff structure, but is subject to deformation. This is in contrary to a notion, that the organ of Corti vibrates as one rigid structure. The most profound deformation appears to occur around outer hair cells, leading to length changes of the reticular lamina. This study provides an important insight into the passive mechanics of the organ of Corti, which seems to be optimized for stimulating inner hair cells as the primary auditory receptors.

LIST OF PUBLICATIONS

This thesis is based on following papers. They will be referred to by their Roman numerals (I-III).

I. Tomo I, Le Calvez S, Maier H, Boutet de Monvel J, Fridberger A, Ulfendahl M. (2007) Imaging the living inner ear using intravital confocal microscopy. *NeuroImage;* 35(4):1393-1400.

II. Fridberger A, Tomo I, Ulfendahl M, Boutet de Monvel J. (2006) Imaging hair cell transduction at the speed of sound: dynamic behavior of mammalian stereocilia. *Proc Natl Acad Sci U S A.*; 103(6):1918-23.

III. Tomo I, Boutet de Monvel J, Fridberger A. (2007) Sound-evoked radial strain in the hearing organ. *Biophys J.* 93(9):3279-84.

Other publications not included into the thesis*:*

Von Tiedemann M, Fridberger A, Ulfendahl M, Tomo I, Boutet de Monvel J. (2006) Image adaptive point-spread function estimation and deconvolution for in vivo confocal microscopy. *Microsc Res Tech. 69(1):10-20.*

Jacob S, Tomo I, Boutet de Monvel J, Fridberger A, Ulfendahl M. (2007) Rapid confocal imaging for measuring sound-induced motion of the hearing organ in the apical region. *J Biomed Opt. 12(2):021005.*

CONTENTS

LIST OF ABBREVIATIONS

BM	Basilar membrane
CLSM	Confocal laser scanning microscope
CNS	Central nervous system
dB	Decibel
GP	Guinea pig
Hz	Hertz
IHC	Inner hair cell
MET	Mechano-electrical transduction
NIHL	Noise induced hearing loss
OHC	Outer hair cell
OoC	Organ of Corte
Pa	Pascal
PTS	Permanent threshold shift
RM	Reissner's membrane
RL	Reticular lamina
ROS	Reactive oxygen species
s.c.	Sub-cutaneous
SPL	Sound pressure level
TM	Tectorial membrane
TTS	Temporary threshold shift
3-D	Three dimensional

1 INTRODUCTION

In humans, as well as in many other living creatures, the analyzing ability of the ear spans an amazingly broad frequency and intensity range, hardly parallel with other sense modalities. The ear is capable of detecting motions of atomic dimensions and respond up to 100 000 times a second in some species (review, Hudspeth 1989). It is thus no wonder, that the quest to decipher the morphological and functional mechanisms of this fascinating sensory organ has driven the curiosity of generations of researchers and clinicians. So, how does the ear's work really work?

1.1 THE EAR - GENERAL FACTS

A human ear can be schematically divided into three functionally differing, yet closely interconnected parts - the external, middle and inner ear.
The external ear consists of the auricle (pinna), the external auditory canal and the tympanic membrane. The role of this system is to locate the sound, concentrate and transfer it on into the middle ear. The middle ear is an air filled cavity containing a chain of ossicles, middle ear muscles and Eustachian tube. Three interconnected ossicles – the malleus, the incus and the stapes are the smallest bones in the human body. By an ingenious lever mechanism they bridge over the tympanic membrane with the oval window membrane of the cochlea. This is to enhance a transformation of the sound wave from a low-impedance, air environment of the external ear into the high-impedance, fluid filled inner ear. The inner ear is composed of the end organ receptors for hearing (cochlea) and equilibrium (vestibulum). Containing very delicate structures of microscopic size, for increased protection it is encapsulated in the hardest bone of body - the temporal bone.

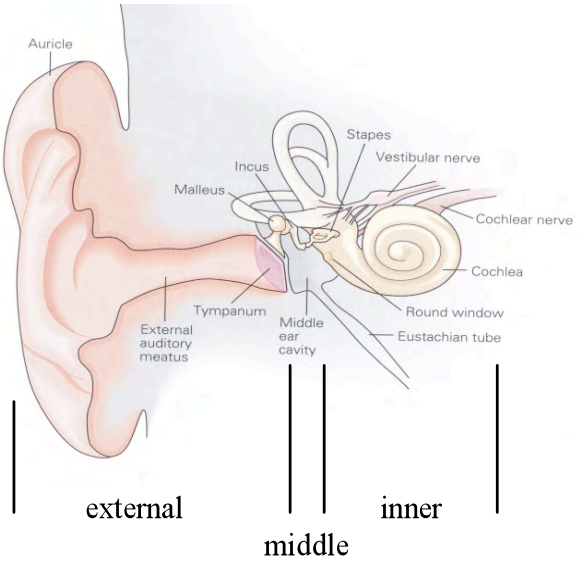

Figure 1; An illustrative side-view image of the human ear and its major constituents. (adapted from Noback 1967)

The piston-like motion of the footplate of the stapes inserted into the oval window further transfer mechanical energy resulting in production of pressure waves, which evokes vibrations inside the cochlea. This evoked vibration is registered by sensory hair cells housed in the organ of Corti, which are capable of transforming mechanical energy into electrical impulses. These impulses in a form of action potentials are then conducted along the auditory nerve all the way to the auditory centers in the brain, which interprets them as a sound sensation.

1.2 THE COCHLEA

The mammalian cochlea is a fluid-filled, coiled structure shaped as a snail's shell. In adult humans the cochlea reaches a size of a chickpea, with roughly 2.5 coils and the total length of 35mm. The cochlear capsule consists of hard, laminar bone, while its interior is comprised of a series of membranous canals filled with fluids of different ionic content.

Three adjacent compartments (scala vestibuli, scala media and scala tympani) can be distinguished, as they coil up together around a bony modiolus, from the base to the apex of the cochlea. Scala vestibuli and scala tympani communicate with each other through a small opening in the cochlear apex - the helicotrema. The Reissner´s (RM) and basilar (BM) membranes separate the scalae from each other. The basilar membrane has a different width and stiffness - being broadest and most rigid in the basal turn and thin and floppy in the apical one. Reissner´s membrane is a simple, double cell layer structure, uniform throughout the whole length of cochlea. Scala media contains endolymph, an intracellular fluid with high potassium (K^+) and low sodium (Na^+) concentration (Smith et al 1954).

Scala vestibuli and scala tympani are both filled with perilymph, containing high Na^+ and low K^+ ions in concentrations typical for extracellular fluids. Scala media or the cochlear duct is housing the organ of Corti (OoC), which is positioned sitting directly on the basilar membrane. From the histological point of view the organ consists of several kinds of supporting cells, nerve endings and two classes of sensory cells – the inner and the outer hair cells.

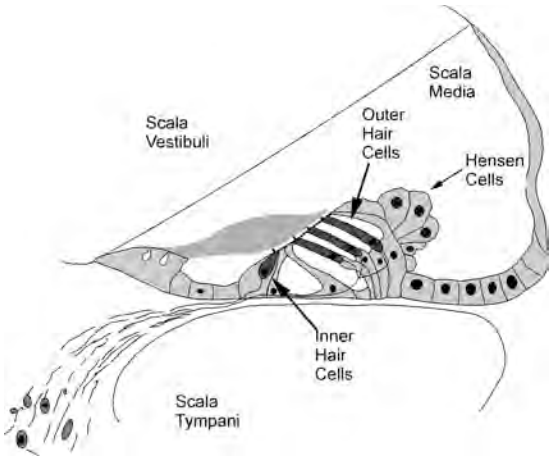

Figure 2; A schematic drawing of the scala media containing the organ of Corti in a cross-section view.

Supporting cells such as Deiters cells, Hensen's cells and inner and outer pillar cells are considered essential in retaining the structural integrity of the hearing organ at rest and during sound stimulation (e.g. Flock et al 1999). The upper surfaces of the hair cells (cuticular plates) and the ones of the supporting pillar cells form together a compact structure termed the reticular lamina (RL). The reticular lamina is from above covered by the tectorial membrane (TM), which is an inert, gelatinous structure, anchored only on its medial edge to spiral limbus. Inner hair cells (IHC) are the genuine sensory receptors, while the outer hair cells (OHC) boost their performance by electromechanical feedback. Outer hair cells are considered to be sensory effectors, as they are capable of changing their length and stiffness depending on the changes in electrical potential (Brownell et al 1985). Additional to their detector function they also generate force, which feeds into the whole system, thus increasing its resulting auditory sensitivity and frequency selectivity (reviews, Fettiplace and Hackney 2006, Dallos 2008). The total number of all hair cells in the human ear is around 15 000, compared to only 9500 in guinea pigs. Each organ of Corti contains one row of inner hair cells and from three to five rows of outer hair cells, depending on their position within the cochlear turns. The same apply for the differences in shape of the OHC. In the basal parts of cochlea three rows of short (25µm), cylindrical OHC can be found, as opposed to four or five rows of taller (70µm) cells represented in the apex. Outer hair cells usually have 6-7µm in diameter. Inner hair cells share more-less the same, flask like shape and size (35µm in length and about 10µm in diameter) independent on their position within the cochlea. They connect to about 90% of all afferent nerve terminals, belonging to the neurons in the spiral ganglion. Only remaining 10% reach to manifolds numerous OHC (Spoendlin 1972). This ratio illustrates also the exclusivity of the IHC as primary sensory analyzers. The OHC on the contrary receive much stronger efferent innervation, supporting thus their role as feedback effectors (Galambos 1956). The apical protrusions of hair cells, known as stereocilia are the primary locations of mechano-electrical sound transduction. They are composed of actin filaments, closely packed together for increased rigidity (Flock and Cheung 1977). Stereociliary arrays atop each hair cell are of variable length (1-4µm) and thickness (100-300nm), interconnected in two to four rows and lined up in increasing sequence from the shortest to the longest bundle, in a formation resembling a staircase. They project upwards from the reticular lamina towards the gelatinous tectorial membrane and are bathed in endolymph. This unique morphological organization of hair bundles is crucial for directional sensitivity in sterociliary deflection (Flock 1965, Hudspeth and Corey 1977), which is a triggering mechanism in the chain of reactions, resulting in final sound perception. Stereocilia of the outer hair cells are firmly embedded into the lower surface of the tectorial membrane, while the inner hair stereocilia are freestanding and lack direct contact with TM (review, Lim 1986).

1.3 PHYSIOLOGICAL BACKGROUND

Sound in a physical sense can be characterized as a wave of periodic air pressure fluctuations, which upon their impact on the tympanic membrane puts it into vibratory motion. The chain of middle ear ossicles then conducts this motion further. Conjunct with the eardrum on one side and connected to the oval window of the cochlea on the other, they enhance transformation of the sound wave from low impedance air environment of the external ear into the high impedance fluid filled inner ear. This high transformation effectivity is based on the favorable ratio between the large tympanic membrane and the smaller oval window membrane, the lever mechanism of the middle ear bones and the buckling motion of the eardrum during sound stimulation (review, Merchant et al 1997). Oscillatory inward and outward motion of the stapes footplate placed over the oval window leads to a movement of cochlear fluids and cochlear partitions. This gives rise to a wave of displacement on the basilar membrane traveling from the base towards the apex of cochlea (von Békésy, 1960).

Owing to gradients in the size and stiffness the traveling waves reach their peaks on different regions of the basilar membrane, depending on the frequency of the stimulus sound. High frequency sounds will produce waves which peak in the basal region of the cochlea, while low frequency stimuli reach their maximum amplitude waves in the apical parts. Each position along the basilar membrane thus corresponds to a particular frequency, termed the characteristic or best frequency, for which the wave amplitude is maximal for a stimulus of given amplitude. Georg von Békésy postulated this traveling wave theory as a result of his pioneering work, using dissected temporal bones for BM vibration pattern measurements. Since these experiments were performed on a dead specimen, it is assumed that the results of his classical work reflect the passive mechanics of the cochlea, which dominates at high sound levels.

The frequency selectivity feature of the basilar membrane plays a major role in sound analysis, as the mechanically sensitive organ of Corti is positioned directly on the basilar membrane. The vibratory motion of the hearing organ induces a complicated interplay of involved structures situated between the basilar and the tectorial membranes. The different modes of vibration of BM and TM result in shearing motion between reticular lamina and tectorial membrane (Ulfendahl et al. 1996a). This shearing leads to a deflection of hair bundles atop hair cells, triggering thus a process of mechano-electrical transduction. The shearing motion theory as a backbone of cochlear mechanics is founded in anatomy and by indirect measurements. However, a direct stereociliary motion measurement is needed in order to decipher the details of sound induced micro-mechanics within the cochlear partition (paper II).

Directionally sensitive deflection of hair bundles opens mechanically gated transduction channels in the apical region of stereocilia, which are immersed in high K^+ endolymph. Through the opened channels K^+ ions rapidly enter the hair cell body, causing its depolarization (Corey and Hudspeth, 1979). Depolarized inner hair cells releases neurotransmitter into the synapse of auditory nerve, which evokes action potential and causes excitation of the afferent nerve, conveying further the sensory information to be registered in the higher auditory centers of the CNS.

1.4 STEREOCILIARY MOTION

The hair bundle is the site of mechano-electrical transduction, which triggers chain of reactions, at the end of which the auditory sensation is registered in the brain. Deflection of the bundle in direction towards the tallest stereocilia opens mechano-electrical (MET) channels positioned at their tips. These ion channels were thought to belong to fast reacting, transient receptor potential family (Corey et al 2004). However subsequent experiments did not confirm this theory (Kwan et al 2006) and so the exact character of the MET ion channels remains unknown up to this day.
Displacement in the opposing direction leads to the closing of MET channels. The hair bundle displacement amplitude is in the range of nanometers at minimum auditory threshholds and is thought to be similar to that of the basilar membrane (Hu et al 1999). Hair bundles never stay still and permanently oscillate around their resting position, modulating thus the probability of opening state of the MET channels, which evokes electric stimulation, perceived finally in the CNS as a sound.
As to the stimulation, which results in a hair bundle deflection, there are major differences between IHC and OHC. The OHC have their stereocilia firmly embedded into the lower surface of tectorial membrane (TM), deflecting thus upon the shearing motion of the TM. In contrast, stereocilia of the IHC are not directly connected with TM and are probably stimulated by a draft motion of the surrounding fluid (Dallos et al 1972). This theory was suggested a long time ago, however no conclusive evidence in a form of visualization of sound-induced motion and its quantification measurements was available. It is only the technique described in our paper II, which for a first time ever provided the convincing data set to actually confirm this suggestion. During these direct measurements we compared the motion patterns acquired from both types of hair cells in the identical region of the cochlear apex. The results showed that sound-induced hair bundle deflections are larger in the OHC then in the IHC. When compared to overall vibration motion of the organ of Corti the outer hair cell stereocilia deflect by $\approx 1/3$ of the displacement of the hearing organ. The IHC stereocilia motion showed 44° phase lead over the displacement of the reticular lamina. The apical turn IHC thus respond to a combination of displacement and velocity near their best frequency, which confirms the notion that stimulus causing IHC deflection is a fluid draft in the sub-tectorial space (paper II, Nowotny and Gummer 2006). While the passive tuning is based on longitudinal gradients in the stiffness of the BM and dimensions of the cochlear partition (von Bekesy, 1960), the active tuning or amplification has an active input from OHC. OHC can produce force by longitudinal contractions of their cell body, driven by changes in electrical potential (Brownell et al 1985). This involves a membrane protein, prestin (Zheng et al 2000). Alternative mode of amplification arises from force generated by the hair bundles (Crawford & Fettiplace 1985) based on the MET channel gating. This mechanism is believed to be especially effective at high frequencies (Fettiplace and Hackney 2006). Detailed mechanisms of the stereociliary micro-mechanics or information, how different structures of the organ of Corti move with respect to each other during sound induced vibration, are not fully understood, mainly due to a lack of direct measurements of their motion patterns.

1.5 EFFECTS OF THE ACOUSTIC OVERSTIMULATION

Exposure to intense sound is known for a long time to result in both functional and morphological changes in the inner ear. This fact has been frequently used in experiments to study various aspects of the noise-induced hearing loss (NIHL) in different biological models. Existing literature on acoustic injury suggests two different stages in the development of the NIHL; a temporary threshold shift (TTS) and a permanent threshold shift (PTS). TTS represents the earlier and reversible phase of the hearing impairment, which is characterized by the structurally reparable changes in the stereocilia such as disarray (Mulroy and Whaley 1984, Tsuprun et al 2003), loss of tip links (Zhao et al 1996, Husbands et al 1999) and depolymerization of rootlets (Liberman and Dodds 1987). Exitotoxic effects on neural elements by substances such as glutamate (Puel et al 1998) in the IHC result in their vacuolization and swelling of afferent peripheral terminals (Spoendlin 1971, Robertson 1983). Functionally is TTS believed to be a result of a temporary closure of outer hair cell mechanoelectrical transduction (MET) channels, which produces a drop in the mechanical sensitivity of the organ of Corti (Patuzzi 2002), due to disruption of the active process provided by outer hair cells (Fridberger at al 2002b). Changes in supporting cell structure have also been reported (Flock et al 1999, Nordmann et al 2000), however these structures appear to be more resilient as compared to the hair cells. PTS as a terminal NIHL stage is irreversible and leads to permanent damage to stereocilia and hair cell loss, as they are considered to be the most vulnerable elements of the cochlear duct (Liberman and Kiang 1978). Damage to OHC stereocilia (especially those in the first row) is almost always worse than that seen in adjacent IHC areas (Robertson 1982, Liberman and Dodds 1984). Loss of outer hair cells leads to elevated hearing thresholds (up to 40 to 60-dB threshold shift, when only the OHC are missing). Functionally the most profound effect is the ceasing of ”active” cochlear mechanisms, characterized by loss in hair cell sensitivity and receptive field (tuning curve) selectivity, along with disappearing of compressive nonlinearity. It is suggested (Cody and Russel 1988) that the outer hair cell is the target of overstimulation (Fridberger et al 1998**)** based on mounting evidence that ”active” processes associated with this cell are responsible for sharp tuning in the inner ear. The outer hair cells are also critical to the frequency-analytic properties of the cochlea (Saunders et al. 1991).

Hair cell receptor potentials following exposure to intense sound thus show elevation in hearing thresholds as a sign of decreased sensitivity. At the same time the tuning curves became broader (less sharply tuned) reflecting thus their decreased frequency selectivity.

Structural damage to stereocilia develops very rapidly, following high intensity (125dB SPL) pure-tone exposures (3.0 kHz). Already after 2 min of exposure the guinea pigs showed stereociliary defects in a form of displacement, fracture, membrane gaps and fusion to the stereocilia on the first row of outer hair cells. Relatively few inner hair cells were involved. As exposure duration increased, these stereocilia injuries became more apparent and spread to outer hair cell rows two and three and the inner hair cells (Thorne et al 1984, Thorne and Gavin 1985, Thorne et al 1986). Corresponding

changes have been observed in the hair cell bodies, following almost identical sequence of their onset. They manifest initially with overall swelling of the hair cell, rounding up, swollen nuclei, vacoulization and terminal bursting up and dying (Fredelius 1988, Wang et al 2002). The relationship between hair cell loss and hearing impairment has proven difficult to establish, because of an inherent variability in cochlear susceptibility to acoustic injury (Saunders et al., 1985). Different types of acoustic exposures produce different signatures of inner or outer hair cell damage along the cochlear partition. These patterns, moreover, appear to be species-specific (Hamernik et al., 1984). In guinea pigs a high-intensity impulse noise damaged mainly the outer hair cells (Rydmarker et al., 1987). Continuous-filtered noise appeared to selectively damage only inner hair cells (Engström et al., 1983). Wideband noise at very high intensity showed a distribution of inner and outer hair cell damage that varied with cochlear location (Engström et al., 1981) When the guinea pig was exposed to the moderately intense pure tones, the damage was localized to the outer hair cells. However, as the exposure level increased, the lesion spread to the inner hair cells (Fredelius et al., 1987). The cellular basis of the NIHL is associated with oxidative stress and increased levels of reactive oxygen species (ROS), toxic free radicals and local increase in calcium concentration (Fridberger et al 1998b), which have been shown to play significant role in noise-induced hair cell death (Henderson et al 2006).

2 AIMS OF THE PROJECTS

Project I: To establish in-vivo imaging method for confocal visualization of the cochlea within undisturbed integrity of the living organism, with its blood and nerve supply still preserved.

Project II: To develop the confocal microscopy based method for rapid imaging of the stereociliary motion, evoked by sound stimulation at in-vitro GP temporal bone preparation in order to study the micro-mechanic behavior of stereocilia in both IHC and OHC.

Project III: Came as a result of technical improvements applied to the method used in project II, which yielded in faster acquisition times, broader stimulus sound frequency range and increased accuracy in motion estimation of the sound-induced deflection patterns of stereocilia in both sensory cell types.

3 METHODS

3.1 ANIMALS

In all our experiments we have used pigmented guinea pigs. The reason for choosing this particular experimental species was anatomical closeness to the structure of human cochlea and relatively easy surgical access. While in humans the inner ear is embedded firmly within the temporal bone, in guinea pigs it is freestanding in a hollow auditory bulla, which is only around 1-2mm thick. Thus after opening the bulla, the cochlea is easily available for imaging, without need for tedious bone drilling, which by itself can cause auditory damage by trans-cranial noise and vibration (Zou J. et al 2001, Sutinen et al 2007). All animal experiments presented here were approved by the local ethics committee and carried out in accordance with its regulations.

3.2 CONFOCAL MICROSCOPY

Confocal laser scanning microscopy (CLSM) has brought a revolutionary change into the field of biological imaging since its introduction in the early 1990-ties. The key advantage of the method is its possibility to look deeper inside the biological tissue.
By blocking the light signal coming from above and under the focal plane, before it reaches detectors, it provides detailed image of the structures within the plane of our interest. This feature, known as the optical sectioning (review, Pawley 1995) enables imaging of the living specimen without need for actual physical sectioning or previous chemical processing.
The approach is particularly beneficial when imaging complicated, fragile, three-dimensional structures, rendering it the method of choice for cochlear visualization.
All our experiments were performed using Carl Zeiss LSM510 Axioplan 2 upright laser scanning confocal microscope, equipped with water immersion lenses of varied optical and size characteristics, as required by the imaging conditions in our different experimental settings. In the project I (in vivo) the tight conditions of animals skull and overall restrained maneuvering space forced us to use a custom built objective lens. This conical shape lens has a pointed tip of 2.4mm diameter, 25x magnification, numerical aperture 0.45 and working distance of 2.18mm (Mayer et al. 1997). Other two in-vitro studies were performed using standard Carl Zeiss lenses with 40x magnification and numerical aperture of 0.8.

3.3 FLUORESCENT DYES

To be able to depict details of biological structures by a confocal microscope, it is necessary to label them first with the appropriate fluorescent dyes. These chemical

substances get into excited state upon contact with light of certain wavelength and are themselves capable of emitting fluorescent light of longer wavelength, than the original stimulus. Resulting fluorescent signal can be subsequently registered at photo-multiplyer detectors of the confocal system.

A broad variety of different dyes are commercially available to delineate not only the cellular structures, but also the organelles and their eventual constituencies. Particularly valuable in the biological imaging are so called vital fluorescent dyes, which only label the living structures, and are thus indicators of viability of the preparation. The probes used in our experiments belong also into this group. The combination of a green, cytoplasmatic dye calcein/AM (labeling the cytoplasmatic compartments of the cells) and a red, potentiometric probe RH 795 (which selectively stains cell membranes of the hair cells and neurofibres), proved to be particularly reliable and successful upon their use at both in-vitro and in-vivo conditions.

3.4 SURGICAL APPROACHES

Biological tissues used in research can be generally divided into in-vitro and in-vivo preparations. In vitro preparations represent situation, when tissue is studied after being removed from the integrity of its host organism, although kept in resembling artificial conditions. In vivo approach, on the other hand reflects more faithfully physiological conditions in the complex environment of undisturbed biological system. Obviously, this approach is much more desirable, yet usually much more laborious and challenging from the surgical point of view.

3.4.1 In vitro preparation (papers II + III)

Isolated guinea pigs cochleae were used for dynamic confocal imaging studies, as they provide superior optical access and high level of stability during the imaging session. The temporal bone was rapidly dissected after decapitation, the auditory bulla opened and glued onto plexi-glass holder, which was submerged into endolymph-like solution (paper II) or tissue culture medium (paper III) filled chamber. A scalpel was used to thin down the bone covering scala tympani compartment in the basal turn of cochlea. A small hole was then drilled through thinned bone, to allow for insertion of fine silicon tube to establish a perfusion system. Another, larger bone-window was made by a fine needle in the cochlear apex, in order to allow the perfusion fluid outflow and also to enable confocal scanning in the region. Syringe filled with oxygenated tissue culture medium mixed with fluorescent probes was attached to the tubing and elevated above preparation to facilitate perfusion. After loading the organ of Corti with fluorescent dyes via perfusion system and mounting firmly the preparation chamber on the stage of microscope the imaging session could begin.

3.4.2 In vivo preparation (paper I)

Pigmented guinea pig was deeply anaesthesized using ketamine (40 mg/kg s.c.) and xylazine (10 mg/kg s.c.), fixed in supine position and tracheotomized. The basic body functions were monitored by electrocardiogram. The body temperature was maintained and measured throughout the surgical procedure.
The mandible was dissected and its posterior parts removed together with the soft tissues, to expose the auditory bulla from underneath. The pinna and external auditory canal were surgically removed with exception of a soft tissue flange strip for attaching of the sound-stimulation speaker. The head of the animal was firmly attached to a custom made holder and further stabilized by dental cement (GC Fuji I, GC Corp. Tokyo, Japan). The auditory bulla was opened by carefully shaving down its bony wall, while keeping the tympanic membrane preserved available for sound stimulation. The middle ear was exposed, cochlea opened at its apex and base to establish perfusion system, as already described in the section above. Compound action potential (CAP) was used to measure the cochlear function, to make sure, that physiological condition of cochlea is preserved during different stages of surgery. The perfusion tube was connected, middle ear filled with MEM, and fluorescent dyes delivered into the cochlear compartments. Perfusion was remained running throughout the whole length of experiment. Animal was placed under the microscope and cochlear structures imaged using custom made, pointed tip, immersion objective lens.

3.5 SOUND OVERSTIMULATION (PAPER I)

To study effects of the high intensity sound exposure and consequent induced morphological changes in vivo, we have applied continuous sound stimulus for periods of 10 minutes from a speaker (Isophone Germany) connected to a power amplifier. The speaker was directly coupled to the animal ear canal through the plastic tubing, delivering sound of frequencies between 400-600Hz at sound pressures corresponding to 130-142dB SPL at the tympanic membrane. The output sound pressure levels were measured using a Brüel & Kjaer interface module type 7533, input/output module type 3109 and Brüel & Kjaer microphone type 4938 with amplifier type 2669C. The immersion of the middle ear cavity in preparation causes estimated loss of 20-30 dB (Franke et al., 1992), lowering thus the effective stimulus impact on the cochlea to 100 -110 dB SPL.

3.6 RAPID IMAGING DURING SOUND STIMULATION (PAPERS II + III)

One of the shortcomings of the laser scanning confocal microscopy is its relatively long acquisition time, due to the scanning mode of building up the image pixel by pixel.

To acquire an image of standard size (512x512 pixels) takes approximately 1 second, which is much too slow for depicting rapid changes as they occur during sound stimulation. Individual pixels though can be acquired at a very rapid rate and are thus unaffected by motion artifacts. To be able to visualize fast moving structures, namely hair cells and their stereocilia, we have developed imaging methods based on the confocal microscopy and custom made data acquisition software. The technique used in project II is based on tracking the temporal relation between each acquired pixel and the phase of the applied sound stimulus. By coupling a confocal system and AD board of the computer we acquire two sets of images sampled by the voltage. Each voltage sample corresponds to a pixel at a given position within the image. Custom made data acquisition programs are then used to assign a phase value to each pixel in the stack of images. The corresponding pixels are then rearranged into new image sequences. These images contain only those pixels, which were acquired at the same phase of stimulus. By repeating the same process for different phases a full motion cycle can be recovered eliminating thus possible motion artifacts. The sound stimulation was at 200Hz with stimulus levels ranging between 88 and 110dB re 20μPa.

Approach used in project III derived from the previous method, however the process of data acquisition and signal processing was further improved using a Fourier row approach. Assuming, that the motion pattern is periodic, it can be reconstructed by computing the Fourier series coefficients for each pixel along the time dimension.

The previous acquisition system used in project II is based on the search for pixels with approximately same phase temporal relation to the sound stimulus. However, noise in the sound channel influenced the recorded phase, and therefore the reconstructed images did not have an absolutely fixed temporal resolution.

Major technical improvement of the project III technique is the use the pixel clock of the confocal LSM system as a time base for the generation of the sound stimulus. This ensures synchronization between image acquisition and stimulus generation. The phase of the sound stimulus for each pixel is then saved and used for Fourier series extraction. This new image sampling technique and the noise-free phase extraction yield less artifacts in the reconstructed images due to the low-pass filtering of the time series and an absolutely fixed temporal relation between images and stimulus. Resulting is substantially faster image acquisition with reduced noise levels and improved motion estimation as compared to the method used in project II. Using the Fourier approach it is possible to acquire full-size images of 512x512 pixels at stimulus frequencies ranging from 100-500Hz.

3.7 THE OPTICAL FLOW METHOD (PAPERS II+III)

The crucial step in an interpretation of dynamic processes imaging is to characterize and quantify the displacement between different depicted structures. Optical flow method, based on the discrete wavelet transforms, was developed to measure the motion pattern of every single pixel within the full sequence of images (Fridberger et al 2004). The approach stems from basic assumption, that pixel intensity remains relatively stable during the whole motion cycle. Optical flow software was custom made in the Matlab (the Mathworks, Natick, MA) programming environment. A sequence of raw images is initially processed by filtering with three-dimensional

Gaussian filter, before the final optical flow algorithm is calculated. Resulting is an optical flow vector, which gets calculated for each individual pixel and faithfully represents the direction and amplitude of its motion (Jacob et al 2007). These vectors can be then compared for different structures, allowing us to estimate different parameters important in the study of the passive micro-mechanics of the organ of Corti and its individual cellular constituents. To confirm reliability of the technique a number of calibration experiments have been performed, which sustained a high level of faithfulness.

4 RESULTS

4.1 PAPER I

CLSM permits detailed visualization of structures deeper inside thick, fluorescently labeled specimens. It is thus possible to investigate living cells inside intact tissue without prior chemical fixation and sectioning of the sample. Isolated guinea pig temporal bones have previously been used for confocal experiments in-vitro, but tissue deterioration limits their use to approximately 3 hours after the death of the animal. In order to preserve the cochlea in an optimal functional and physiological condition, we have developed an in-vivo confocal model using living, anaesthetized guinea pigs. This microscopic method for the inner ear visualization faithfully reflects the integrity of the living organism, including the regenerative processes and may be in experimental conditions used for relatively long time.

In spite of tedious and timely surgical procedure, as well as numerous technical challenges due to sub-optimal imaging conditions, this approach yielded images of comparable quality and detail to the ones acquired from in-vitro cochlear preparations. Illustration of this fact can be seen in Figure 3, which represents the cross-sectional view of the hearing organ, as it is visualized from above through the intact Reissner's membrane.

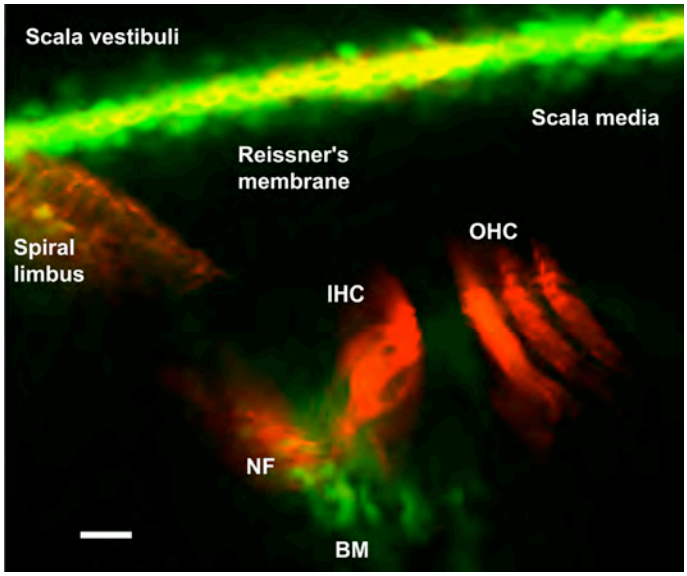

Figure 3; An overview of the hearing organ with outer hair cells (OHC), inner hair cells (IHC) and nerve fibers (NF) labeled red by RH 795. Basilar membrane (BM), supporting cells and Reissner's membrane stained green with calcein/AM. Scale bar, 20µm.

The Reissner's membrane depicted in green is overlying the hearing organ with nicely resolved red rows of inner and outer hair cells. Individual hair bundles protruding from the apical surfaces of both types of the hair cells can be distinguished. Parts of the basilar membrane supporting the organ of Corti are also visible, stained in green. The lower (medial) side of the Reissner's membrane is shown and individual cells of this double-layered structure can be identified. Supporting cells delineating the inner spiral

tunnel along with the interdental cells of the spiral limbus are all marked in green. Brightly red stained cochlear nerve fibers, as they cross the inner sulcus area and attach to the inner hair cells, as well as the cell membranes and cuticular plates of the first row of outer hair cells can be seen. The spiral limbus is also well depicted in red as a mesh of filamentous structures passing along the teeth of Huschke, whereas the interdental cells are only very faintly stained in green.

To delineate subtle, living cellular structures within the cochlea a previous fluorescent staining is necessary. Decision to use the same combination of vital dyes, as the one already proven successful during our in-vitro cochlear visualization experiments, showed to be correct. The most useful labeling in our living animal experiments proved to be a combination of styril dye RH 795 and calcein/AM ester. The red staining RH 795 is a lipophylic dye that was originally designed to measure membrane potential differences. As previously described in many in-vitro studies in cochlea, RH 795 preferentially labels the sensory cell membranes and neuronal fibers, while staining of the supporting cells is much weaker (Flock et al. 1999). Illustration of this staining pattern can be seen in Figure 4, which is showing a higher magnification profile view of the hearing organ.

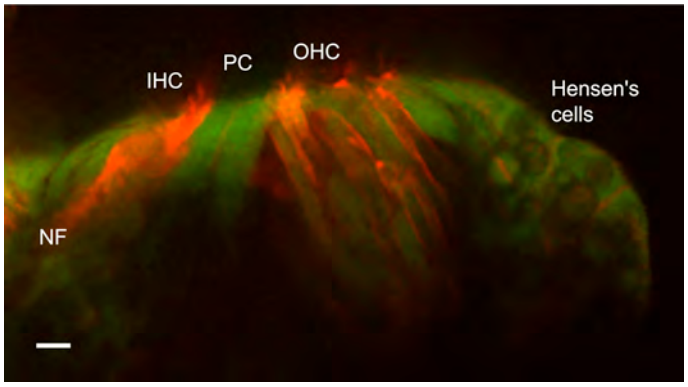

Figure 4; A profile view of the organ of Corti at higher magnification (Scale bar 20µm). Nerve fibers (NF), sensory cells (IHC and OHC) and supporting cells (e.g. pillar cells, PC and Hensen's cells) are readily identified (same dyes used as in Fig. 3)

The cell membranes of both inner and three rows of outer hair cells, along with nerve fibres are clearly seen labeled red by the RH 795. Even individual hair bundles of both hair cell types are nicely depicted in red, as they protrude from their apical surfaces.
Calcein/AM ester is a vital dye, which after undergoing enzymatic cleavage in the cytoplasm of the living cell provides green staining. So the cytoplasmatic compartments of the supporting cells and cells along the reticular lamina are stained in green as also seen in the Figure 4. Notable are also nicely delineated, round shaped, dark lipid droplets inside the cytoplasm, so characteristic for the Hensen´s cells, which can be identified on the lateral border of the OoC. A morphological aspect of the study reveals the similar labeling patterns and preferences of the applied dyes (RH 795 and calcein/AM), as previously observed in the temporal bone preparation. The identical loading sequence of the fluorescent dyes, and the succession in which they gradually stained different cochlear structures, indirectly also reconfirmed the viability of our previously established temporal bone in-vitro imaging models. Intense sound applied to the animal ear during the sets of living animal experiments has caused morphological changes, comparable to the ones, described in the temporal bone (in-vitro) studies resulting in noise-induced cochlear damage. Images taken before and after the acoustic overstimulation from the same cochlear location are presented in the Figure 5.

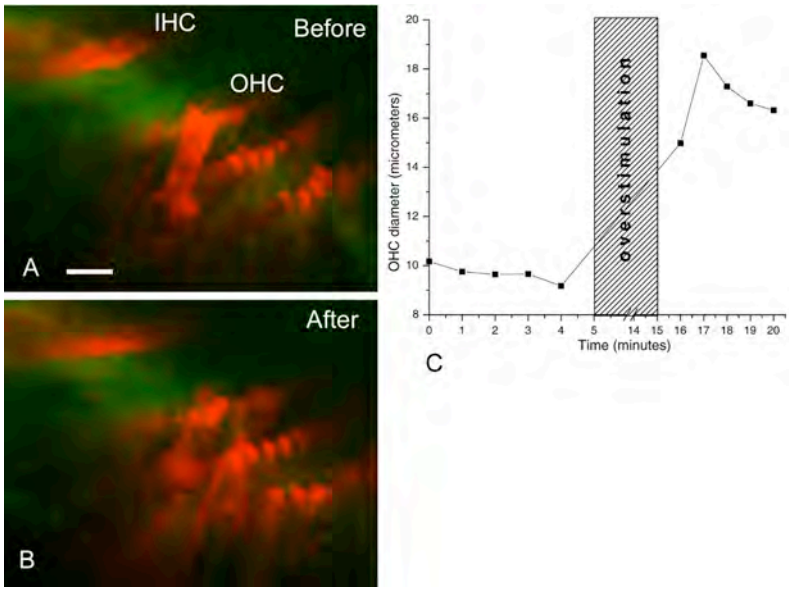

Figure 5; Outer and inner hair cells depicted before (A) and after (B) the sound overstimulation (500Hz at 130dB SPL for 10minutes). Sensory cells (OHC and IHC) are seen in red (RH 795), supporting cells in green (calcein/AM). Swelling of the OHC and disarrangement is notable (Scale bar 20µm). The change in diameter of the OHC after acoustic trauma vs. time (C)

A 500Hz sine wave sound at 130dB SPL applied for 10 minutes led to a distinct change of the outer hair cells shape as well as disarray in cytological architecture of the hair cell rows. A typically slender, prolonged cylindrical outer hair cell body (as seen delineated in red by RH 795 in 5A) was observed to swell, increase its diameter, round up (5B) and finally burst and die. Inserted graph in Figure 5 C illustrates the gains of the OHC diameter after the overstimulation as the cell lost its homeostasis and began to swell. No major morphological changes were noticed in green stained supporting cells, which are known to be more resistant to noise as compared with the hair cells.

The first row OHC has shown to be the most susceptible to acoustic overstimulation following by second and then third row of the OHC. The last hair cell type to become impaired by applied sound proved to be the IHC. Similar morphological changes, as well as the sequence of their onset in different hair cell sub-populations, were previously observed in temporal bone imaging experiments studying the effects of intense noise trauma.

4.2 PAPER II

Vibratory motion of the cochlear partition triggers conversion of mechanical stimuli into electrical signals. This transduction process depends on deflection of stereocilia atop the hair cells, which then gate mechanically sensitive ion channels. The ratio between the hair bundle deflection and sound evoked vibration of the organ of Corti is critical for further mechanical and neural events underlying sound perception. Precise mechanisms of this complex micro-mechanic interaction, as it occurs during sound stimulation, are yet not fully understood due to a lack of direct measurements.

A new method for confocal imaging of rapidly moving structures was developed to image stereocilia during simultaneous sound stimulation in the apical region of guinea pigs cochlea. A temporal bone preparation is used, which is subject to a direct sound stimulation. The method enables study of a passive motion of various cellular structures of the reticular lamina in the organ of Corti as they move in respect to each other. Results are presented in the form of motion trajectories and quantified by the optical flow method. The accuracy of our measurements was approved by a calibration, using a high-precision piezoelectric translator and a fluorescent target attached to its probe. Calibration test results show, that over the range 0.045-0.7μm the measured motion closely approximated the actual motion of the fluorescent target driven by a high-precision translator. Motion patterns measured in our experiments fall within this range of displacements.

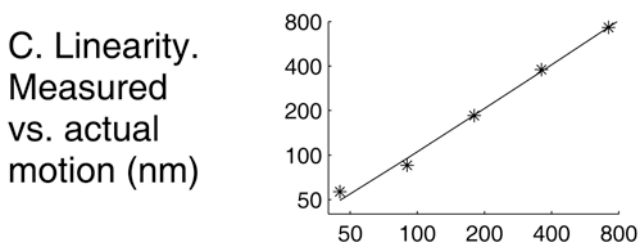

Figure 6; A linear relationship between the high-precision translator driven actual motion (x) and the motion measured by our technique (y).

The technique successfully depicts sound induced motion patterns of the outer and inner hair cell bodies and hair bundles. During stimulation, the outer hair cell bodies moved in phase with the reticular lamina, while the stereocilia deflected in their own pattern. The same is true for the inner hair cells, however with smaller deflection amplitudes.

Hair bundle motion

The hair bundles of the outer hair cells during the sound-induced vibration moved as stiff rods, as their points of attachment to the cell body provided the base for this motion. Such motion pattern depicted in two neighboring outer hair cells from the apical (low frequency) region of the cochlea is shown on Fig 7A.

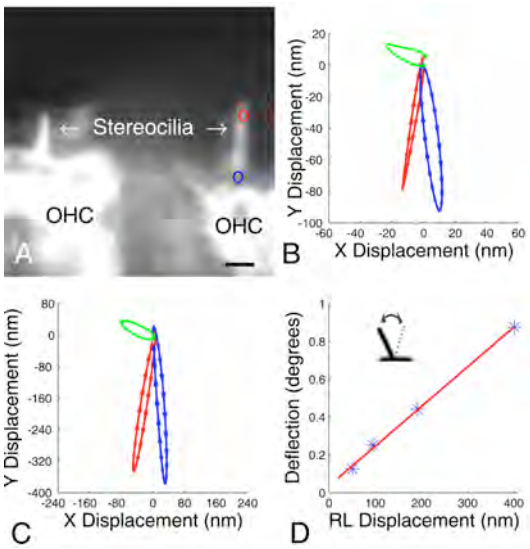

Figure 7; Outer hair cell motion patterns.
(A) Confocal OHC image (Scale bar 3μm) with 2 points of measurements and their corresponding vibration trajectories depicted in the same color. Green vector is a difference between trajectories and represents the hair bundle deflection. Sound stimulation trajectories at 200 Hz with stimulus level of 98 dB SPL (B) and 110 dB SPL (C). Angular deflection vs. RL displacement (D).

The pivot point of the motion, which lays at the attachment of the hair bundle to the cuticular plate of the hair cell is marked by the blue circle. The blue trajectory in Fig 7B illustrates, that motion at this point was directed almost along the long axis of the stereocilium. The tip of the bundle (marked by a red circle in Fig 7A) however moved in different direction as compared to that of the base. The differing motion patterns measured between the tip of the bundle and its base led to a hair-bundle deflection, the size of which was obtained by comparing the difference between the two trajectories. The resulting deflection trajectory was thus computed and is presented in green.
During the down-directed motion of the hair cells toward the scala tympani, the bundle deflected to the left, reaching a maximum of 28nm (Fig 7B). Maximal bundle deflection was in phase with peak displacement of the reticular lamina, downward displacement of the organ of Corti resulting in deflection in the inhibitory direction.
A clear linear relation between the hair bundle deflection of the outer hair cells and reticular lamina displacement was observed in our experiments. The difference in length of different hair bundles obviously plays an important role and therefore needs to be taken in consideration. So angular deflection appears to be more suitable parameter, when comparing deflection of bundles with different length. It is defined as the angle formed between the two extremes of the sterocilia deflection. Angular deflections can be calculated as the arctangent of the ratio between stereocilia deflection and the length of the hair bundle (see also Fig 7D *Inset*). As shown in the Fig. 7D, angular deflections ranged between 0.13˚ and 0.88˚ for the four stimulus levels used here.

Corresponding measurements were also acquired from the inner hair cells (Fig 8A) in the same preparations and spiral locations, while using similar acoustic stimulus levels in order to allow for direct comparison with the OHC results (Fig 7).

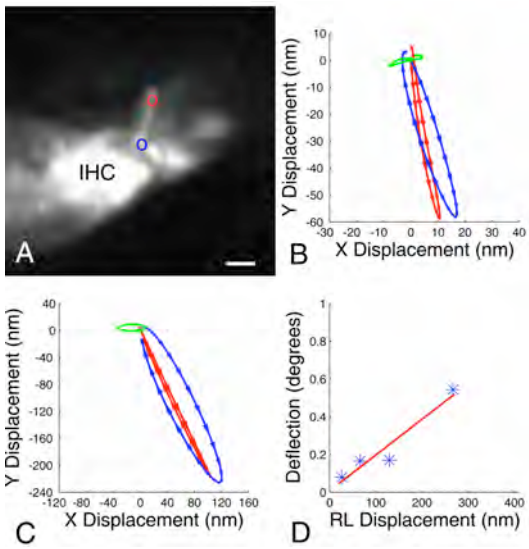

Figure 8; Inner hair cell motion patterns.
(A) IHC confocal image (Scale bar 3µm) and the motion trajectories (as in Fig. 7) at 200Hz sound stimulation with 98dB SPL stimulus (B) and 110dB SPL(C). (D) Angular deflection as a function of reticular lamina displacement.

Distinct differences in motion patterns can be recognized between the inner and outer hair cell trajectories recorded from same spiral location and preparation. The overall direction of motion in the inner hair cells was almost identical at the top and at the base of the hair bundle. It was only more elliptical motion near the stereociliary base as compared to the tip, which gave rise to the bundle deflection. At all stimulus levels, the inner hair cell showed smaller displacements than outer hair cells. In Fig. 3B, the peak-to-peak deflection was 14nm, as compared with 28nm for the outer hair cell. Again, the uneven length in different hair bundles influences the comparison of the total "deflection swing" and therefore the angular deflection is a more reliable measure; angular deflection ranged from 0.08˚ to 0.54˚, or ≈61% of the value found for the outer hair cells (see Fig. 7D and 8D).

Phase and amplitude

Stereocilia of the outer hair cells are embedded into tectorial membrane and thus respond to the displacement of the hearing organ. On the contrary, hair bundles of the inner hair cells are freestanding and lack direct contact with tectorial membrane. The actual motion stimulation of the IHC sterocilia is still not completely resolved issue and thus a one of paramount importance in the field of cochlear mechanics. Recent studies support the interaction with the fluid surrounding the hair bundle as a possible explanation for their motion. Based on these facts a phase difference is expected to occur between inner and outer hair cell stereocilia deflection. Relation between phase and amplitude for hair bundle deflection in both OHC and IHC is depicted in Fig. 9, where it is plotted together with the displacement at the reticular lamina.

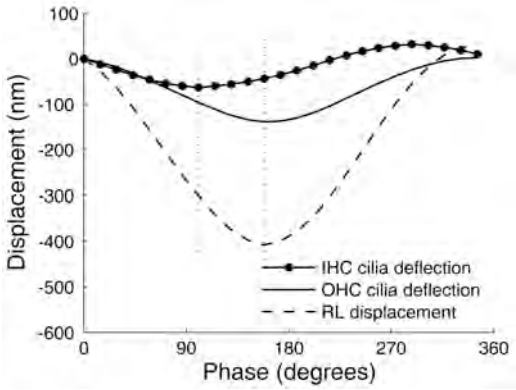

Figure 9; A relation between stereocilia deflection and displacement of the reticular lamina (RL). The deflection phases of identical cochlear position IHC and OHC hair bundles in a phase–match with sound induced motion of the reticular lamina at 104dB SPL.

Predictably, the maximum deflection of outer hair cell stereocilia followed the peak displacement of the reticular lamina. However, this was not the case for the inner hair cell, where maximum deflection occurred before the reticular lamina had reached its peak displacement. The inner hair cell deflection were after performing a Fourier transformation showed to led reticular lamina displacement by 53˚. As response amplitudes and phases vary according to hair cells position along the cochlear spiral, it is necessary for adequate comparison of inner and outer hair cell cilia vibration that the measurements are performed at the identical position. Based on the data from 25 cell pairs from four different preparations, where each pair was located at the same position within the cochlear spiral, the mean phase lead for the inner hair cell bundle deflection was 44˚. The apical turn IHC thus respond to a combination of displacement and velocity near their best frequency, which confirms the notion that stimulus causing IHC deflection is a fluid draft in sub-tectorial space.

A ratio between stereociliary deflection and reticular lamina motion is very important parameter, because it determines the stimulus applied to transduction channels. Hair bundle deflections are in general much smaller than the displacement of the reticular lamina. On average, the ratio between outer hair cell stereocilia deflection and reticular lamina displacement was 0.35±0.12 (mean±SD). For inner hair cells, the corresponding ratio was 0.37±0.13 (the displacement of the reticular lamina was smaller near inner hair cells, making the ratio similar to the outer hair cell value despite the smaller deflections of the inner hair cell stereocilia). So, even though inner hair cells bundles vibrate with smaller absolute deflection amplitudes as compared with the outer hair cells, the “transformer ratio” from reticular lamina motion to stereocilia was the same as in outer hair cells.

A novel confocal microscopy technique for rapid imaging of stereociliary motion during simultaneous sound stimulation was developed. It employs a guinea pigs temporal bone preparation, subject to a sound stimulation in order to reflect the passive motion of the cellular structures of the organ of Corti. We compared the motion patterns acquired from both types of hair cells in the identical region of the cochlear apex. The results showed that sound-induced hair bundle deflections are larger in the OHC then in the IHC. When compared to overall vibration motion of the organ of Corti the outer hair cell stereocilia deflect by ≈ 1/3 of the displacement of the hearing organ.

4.3 PAPER III

The method for the fast imaging of sound induced cellular motion in cochlea, using in-vitro temporal bone preparation (as described in our paper II) was further technically improved by computing the Fourier series coefficients for each acquired pixel along the time dimension. This decreased the pixel brightness variation and consequent resulting noise, while allowing for better motion estimation in the final image sequence reconstruction. Technical developments resulted also in faster acquisition times while

using larger image format (512x512pixels) and increased sound stimulation frequency interval up to 500Hz, which covers the best frequency range of the imaged apical region of cochlea. The larger image format in practice means that acquired pixel size can be smaller, and therefore the resulting image resolution increases as well. This advanced technique was used to depict the motion of both inner and outer hair cells during sound stimulation in moderate levels over the frequency range of 100-500 Hz. Resulting motion patterns are presented in the form of tuning curves, derived from measured vibration trajectories. A set of measurements was performed in 28 guinea pigs excised cochlea preparations and tuning curves were calculated based on this data. An illustration of such curve, taken from the outer hair cell at stimulus frequencies between 100 and 300 Hz is presented in figure 10 B (asterisks). Striking resemblance is noticed in frequency tuning between this preparation (reflecting mostly passive mechanics) and that, which is found in the receptor potentials of apical turn inner hair cells in-vivo (squares, data from Dallos 1986). The slopes of the two curves appear quite similar, especially around their peak regions (10 B). A confocal image complementary to this data set is depicted in figure 10 A. In this particular case, the preparation was subject to sound stimulation at 175 Hz and 93db SPL during the image acquisition.

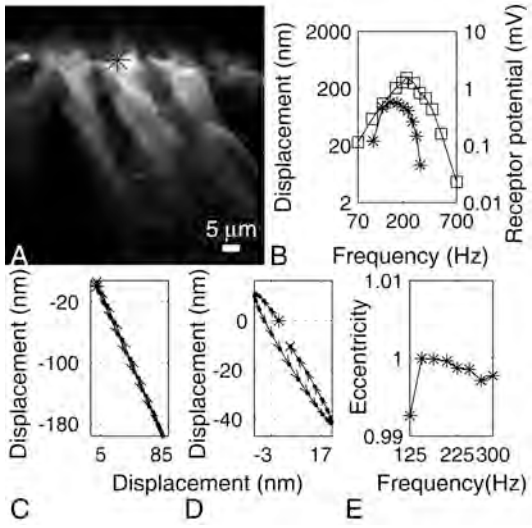

Figure 10; Tuning curves and motion trajectories from a third row outer hair cell. Micrograph of the OHC during acoustic stimulation (A) and its mechanical tuning curve (*) as compared to a fourth turn IHC receptor potential (□) depicted in panel (B). Trajectory at 150 Hz and eccentricity 1 (C). Trajectory at 275 Hz and eccentricity 0.997 (D). Comparison of trajectory eccentricities at different stimulus frequencies presented in panel (E)

The measurement point in the reticular lamina, where the displacement shown in figure 10 B – D was taken at is marked by asterisk. Trajectory in the figure 10 C at 150Hz sound stimulus with eccentricity=1, compared with 10 D trajectory taken at 275Hz stimulus frequency with eccentricity=0,997. The maximal response was measured at 150Hz and best frequencies ranged between 150 and 225 Hz in this data set.

Eccentricity is an important parameter, which can be useful in analyzing trajectories (e.g. the ones shown in the figure 10 C and 10 D) as it provides the means of quantifying trajectory shapes. Calculated by a mathematical formula based on length of trajectory´s major and minor axis the eccentricity represents a dimensionless number, which would be zero for a circle and one for a straight line. Trajectories measured at 150 Hz formed almost perfect lines as the cell moved along a single, well-defined path (fig. 10 C). A different motion pattern was observed at 275 Hz, where motion direction at scala vestibuli (top of the image) occurred along a different path from that seen

during motion toward scala tympani. This gives rise to a trajectory, which begins to resemble oval in its shape (fig.10 D). Figure 10 E illustrates the high eccentricity values in the region around the best frequency and the lower ones on either side of the peak.
Significant differences were found across the entire data set between trajectory eccentricities measured at 125, 150 and 175 Hz and those measured above 250Hz.
All inner hair cells measurements showed a tendency to have lower eccentricity as compared to the outer hair cells.
It was the stimulus frequency, which influenced both the vibration amplitude and the trajectory shape, however this was not the case for the main axis of vibration. The direction of vibrations and resulting trajectory orientations nevertheless remained the same regardless of stimulus frequency, depending strongly on the cell type. The inner and outer hair cells during a sound induced vibration differed in their main trajectory axis as is illustrated in figure 11.

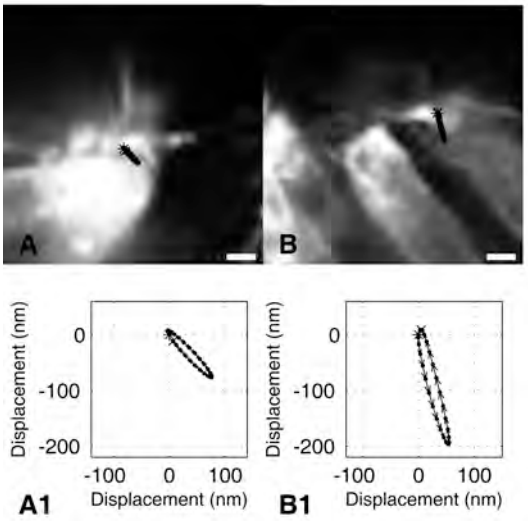

Figure 11; Vibration trajectories of different class hair cells at the same region within the cochlea. Confocal images of the IHC (panel A) and the third row OHC (panel B) acquired from the identical cochlear location (Scale bar 3μm) at 203 Hz and 93 dB SPL stimulus level. Measured sound induced motion trajectories (A1 and B1) corresponding to the images with a scale bar of 150 nm.

The confocal micrograph of the inner hair cell (sound stimulation at 203Hz) can be seen in figure 11 A along with the illustrative trajectory which is 20x magnified relative to the real pixel size (superimposed on the image). The same trajectory is also shown in panel A1 (for comparison with the one taken from OHC in panel B 1). The peak-to-peak displacement of this cell was 70 nm with the trajectory angle of 134˚. The corresponding third row outer hair cell image in figure 11 B was acquired from the same cochlear location as the IHC in figure 11 A and was subject to identical sound stimulation. Nevertheless the resulting trajectory is apparently different from the corresponding one of the inner hair cell. The main axis of the trajectory showed an inclination of 105˚ and the peak-to-peak amplitude was 180 nm. The trajectory orientations differ from each other depending solely on the hair cell type, creating thus a pattern noticed throughout all measured frequencies and intensities. The inclination was observed to shift gradually along the reticular lamina, so that first and second-row outer hair cells had trajectory orientations intermediate between those of inner hair cells and third row hair cells.
According to a traditional view the reticular lamina is a rigid, connective structure linking the apex of the sensory hair cells in a plate-like formation. It was also believed that due to its stiffness it moves jointly as one unbending complex. Surprisingly, these

data show, that adjacent parts of this structure vibrate in dissimilar directions, which obviously results in a deformation. In order to quantify the possible deformation changes all measured trajectories were brought into a common coordinate system, where the reticular lamina was oriented along the horizontal axis of the image. A motion across this axis is defined as being ´radial´, while the vibration component directed perpendicular to the reticular lamina is the `transversal´ one (Fig 12A).

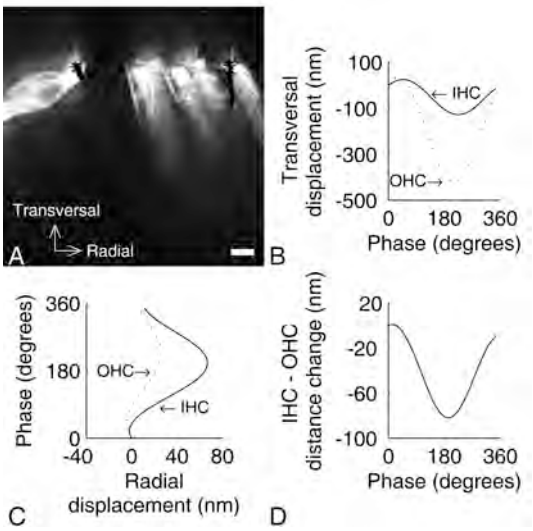

Figure 12; Transverse and radial vibration components in outer and inner hair cells. (A) Sound stimulated (200Hz and 96 dB SPL) hair cells of both classes in a confocal micrograph (Scale bar 10µm). Differences in radial (C) and transversal (B) vibration components in IHC and OHC. The actual distance change (nm) between IHC and the third row OHC (D).

The transversal direction in the inner and outer hair cell sound-induced vibration is presented in Figure 12 B. Apparently the transversal vibration component had substantially higher amplitude in the outer hair cell (dotted line) as compared to the IHC. The corresponding radial motion is depicted in panel 12 C. In contrast to transversal vibration the measured peak-to-peak radial displacement here was 80nm for the inner hair cell, but only 30nm for the outer hair cell. So that means that inner hair cell during downward motion moved further in the direction of the vascular stria, than did the third row outer hair cell. Their mutual distance therefore decreased which consequently led to a compression of the reticular lamina (Fig 12 D). Across the whole data set, the radial vibration component was on average 1.12 times larger in the inner hair cells then in the third rows of outer hair cells. These results confirm presence of deformation of the reticular lamina during moderate level sound stimulation, based on the fact that movements of the opposing ends of the same structure differ in size.

In order to assess a level of mechanical deformation a general parameter has been introduced termed the strain. It is calculated by dividing the length change by the initial distance between the two points. The average strain was 0.1% for the region of the reticular lamina between the inner hair cell and the first row of outer hair cells, while the segment between outer hair cells 1 and 2 showed an average strain of 0.2% and that between outer hair cells 2 and 3 0.3%. The strain values for the segment between the inner hair cell and the first row of outer hair cells were significantly different from that between outer hair cell rows one and two. This set of data also confirms the deformation of the reticular lamina and that most of it occurs near the outer hair cells.

Although primarily focused on a passive mechanics component, this technique may also help to explain other active mechanisms underlying cochlear amplification and may be useful in creating the experimental models of cochlear function.

5 DISCUSSION

The sense of hearing represents one of the principal communication tools in our interaction with the outside world. Due to ever-growing noise levels and other environmental factors the percentage of hearing-impaired or deaf people is constantly on the rise. Up to this day there is no causal treatment available for the inner ear originated deafness. This may be partly due to a rather limited knowledge of the subtle processes involved in the physiology of hearing perception, particularly at the level of cochlear micro-mechanics.

The introduction of the confocal laser scanning microscopy into the hearing research has truly opened a new horizon in the cochlear visualization. Optical sectioning feature of the CLSM allows depicting details of subtle, yet crucial cellular structures of the organ of Corti, both from the morphological point of view (Ulfendahl et al 2000, Flock et al 1999), as well as when it comes to their dynamics and mutual interaction during sound-induced vibration (Fridberger et al 2002 and 2003). Many of these important attributes were previously left undisclosed due to a delicate structure and difficult accessibility of the inner ear.

All papers presented here are introducing the new, original methods for cochlear visualization, based on the confocal microscopy approach, as they were gradually developed in our group. They combine in-vitro dynamic imaging of the guinea pigs temporal bone and the in-vivo animal model for imaging of the inner ear in the living, anaesthetized guinea pig. A depicted anatomical area of the cochlea - the apical turn region, was identical in all our studies. This is due to relative good accessibility for the confocal microscope objective during the image acquisition. At the same time, the apical bone shell needs to be removed anyway, in order to establish a perfusion system to deliver the fluorescent dyes into the cochlea and to allow the confocal image acquisition. This apical confocal imaging approach has a long and well-established tradition in our group (Ulfendahl et al 1996).
We have also used standardized labeling protocols, keeping the same dye combination throughout all experiments, and likewise the surgical and dye-loading procedures were kept similar. Thus the results of our studies complement each other and provide a complex insight into the morphology and functional properties of the organ of Corti from the temporal bone-excised cochlea, up to the novel intra-vital animal model.

Each and one of the methods described here is unique in its capacity and limitations.
The living animal imaging approach represents a cutting-edge visualization technique. It is fully in accord with the current trend in biology, which calls for in-vivo imaging, as near as possible to the physiological conditions. Therefore it provides information on how the imaged organ or structure actually functions inside the undisturbed surroundings of the living organism. Our preparation can be used for relatively long time periods and thus offers a rare opportunity to study even reparatory processes (such as those that occur after a transitory hearing loss). The acoustic overstimulation applied to the imaged ear led to morphological changes, which are consistent with previous data acquired from temporal bone preparations.

The data acquired from living animal model are indeed highly desirable, yet to obtain them comes at a price. The inevitable surgery to gain the access into the cochlea via trans-mandible approach is laborious, timely and bears a risk of possibly fatal bleeding from major blood vessels running through the exposed anatomical area.
The physical opening in the auditory bulla is rather limited in space and needs to be filled with tissue culture medium (required for the immersion objective in order to perform properly during imaging session). The confocal microscope objective also needs to be custom-designed with pointed tip and a longer working distance, which inevitably comes at expense of lower numerical aperture and thus decreased final image resolution. These factors altogether sums-up for rather disadvantageous imaging conditions during the confocal image acquisition session. Therefore different image restoration and processing techniques have been custom developed in our group in order to improve the final image quality (Boutet de Monvel et al 2001).
The periodical breathing motions of the living animal create frequent artifacts, especially when trying to acquire continuous stacks of images (so called z-stacks) in order to gain a 3-D optical effect. Another unsolved problem to reckon with, is how to attach the head of the animal firmly enough to allow for long-term imaging without a major drift, while still retaining the undisturbed breathing. Controlled artificial ventilation may provide a feasible solution for the above mentioned imaging-stability problem issues.
Despite of numerous challenges this intravital, confocal model is expected to enable further study of the subtle cellular and functional mechanisms involved in the mechanical function of the hearing organ. Additionally, it opens new opportunities in investigation of acute acoustic damage, temporary threshold shifts, the role of efferent nerve system and possible recovery of structural changes after noise exposure, which may be of relevance for further clinical and pharmacological research towards the cure of sensorineural hearing loss.

The in-vitro methods using an excised temporal bone of the guinea pigs for visualization are already well established and widely utilized in the field of auditory research (Flock et al 1998). Apart from the laser interferometry experiments (Ulfendahl et al 1996a+b, Ulfendahl 1997) the temporal bone preparations have never been used before for a dynamic confocal imaging of the vibrating organ of Corti during simultaneous sound stimulation. From this aspect the rapid imaging techniques used in paper II and III are both innovatory and revealing. They provide a non-parallel insight into the vibrating mode of the different cell constituents of the cochlea. The laser interferometry is indeed superbly accurate method for measuring the motion pattern of different cellular structures (Willemin et al 1989, Ulfendahl et al 1989, Robles and Ruggero 2001, Fridberger et al 2002b) although it is only capable of following the motion of one point at the time. Our methods however depict the motion patterns of the whole organ of Corti, providing thus the overall picture of the cochlear mechanics in two dimensions.

Deflection of stereocilia is crucial in the process of mechano-transduction, which leads to the production of receptor potentials, transmitter release and action potential in the auditory nerve, later perceived as a hearing sensation. Detailed mechanisms of the hair bundle mechanics and their interaction with neighboring structures during sound stimulation are still not completely known, partially due to a lack of direct visualization

methods. A very important parameter in this regard is the motion ratio between stereocilia deflection and sound–evoked vibration of the reticular lamina. Outer hair cell stereocilia are firmly attached into a gelatinous accessory structure, the tectorial membrane. The different motion patterns between the tectorial membrane and the remainder of the hearing organ, lead to a mechanical interaction via the hair bundles of the outer hair cells, resulting in sterociliary deflection and force production. In the case of inner hair cells the situation is much more complex, as their stereocilia are freestanding and appear to lack firm connections to other parts of the organ of Corti. The mode of their hair bundle deflection remains therefore unclear. Fluid flow around stereocilia is believed to play an important role, however it is not known, how stereocilia deflection is affected by overlying tectorial membrane motion. The only way to address these questions is by direct measurements of stereocilia motion. We accomplished this by our novel confocal imaging techniques, which are capable of capturing high-resolution images from objects moving at several hundreds Hz, something that would not be possible with conventional confocal microscopy.

In our paper II we compared the motion patterns acquired from both types of hair cells in the identical region of the cochlear apex. These results showed that sound-induced hair bundle deflections were larger in the OHC then in the IHC. When confronted to overall vibration motion of the organ of Corti the outer hair cell stereocilia deflect by ≈ 1/3 of the displacement of the hearing organ. The IHC stereocilia motion showed 44° phase lead over the displacement of the reticular lamina. The apical turn IHC thus respond to a combination of displacement and velocity near their best frequency, which confirms the notion that stimulus causing IHC deflection is a fluid draft in sub-tectorial space.

Results of the paper III showed that the passive mechanics of the hearing organ involve fast structural changes that lead to deformation of structures that are often considered as relatively stiff. During moderate-level sound stimulation, the length of the reticular lamina changes. We also demonstrated that the structural alterations appear most pronounced near the outer hair cells. The larger radial vibration component measured at the inner hair cells may be important, since it may contribute to deflection of inner hair cell stereocilia, as they lack firm contact with overlying structures. Although primarily focused on a passive mechanics component, nevertheless both approaches used in paper II and III may also help to explain other active mechanisms involved in cochlear amplification and be useful in creating the experimental models of cochlear function.

We believe, that results of all here presented studies can lead to a better understanding of both physiological function and microscopic structure of the cochlea, as well as to reveal the pathological processes underlying the sensorineural hearing loss. Consequently they may also indirectly contribute to future development of new preventive or treatment strategies against the different forms of deafness.

6 ACKNOWLEDGEMENTS

This thesis is a result of a mutual cooperation of a whole team of colleagues and co-workers affiliated to the Center for Hearing and Communication Research, Karolinska Institute and Karolinska University Hospital in Stockholm, all of whom I would like to express my deep and sincere gratitude to:

Anders Fridberger my main supervisor in this thesis work. Your scientific mentorship, encouragement and support have been truly fundamental to my scientific development. Thank you for your endless patience and explanations during the Mat-lab calculation sessions and critical reading of my manuscripts. You have always been there for me, to provide a good piece of advice, feedback to my writings, to discuss problems and suggest possible solutions to them. Your enthusiasm, profound knowledge in various fields of science and willingness to share it with others has always been a great inspiration to me.

Mats Ulfendahl the director of the Center for Hearing and Communication Research and my co-supervisor for inviting me into his lab and getting me interested and involved into the fascinating world of the auditory research and confocal microscopy. Thank you for the opportunity to work in such a unique group of scientists of diverse fields of expertise and different nationalities, which blended just perfectly to give rise to a spirit of mutual cooperation, fruitful discussion and unrivaled scientific exchange. Your vision, creativity, scientific wisdom and experience impressed me deeply. Without yours always friendly and patient leadership, thoughtfulness, generosity and trust in me I would not be able to accomplish this work.

Jacques Boutet de Monvel my co-supervisor for your friendly help with all the computations, technical issues and patient explanations of the image processing techniques, which you are a real master of. Thank you for your readiness to help at any time and in any issue, from mathematical image enhancing approaches to positive comments and suggestions regarding our mutual papers.

Sophie Le Calvez for practical introduction into the confocal microscopy and related imaging as well as animal preparation techniques.

Hannes Maier for providing a custom-made microscopic lens, his time spent with us during the living animal confocal imaging sessions. Your insightful comments and practical recommendations have many times helped us to move forward in our experiments.

Stefan Jacob and Miriam von Tiedemann for friendship and successful collaboration over the mutual confocal microscopy projects.

Åke Flock for sharing of his extensive knowledge, life-long scientific experience as well as practical skills in the fields of confocal imaging and auditory physiology. It was an honour to be able to interact with you.

Anette Fransson and Paula Mannström for allways reliable laboratory assistance and smooth cooperation.

Louise von Essen for administrative help.

My workplace room-mates Åsa, Miriam, Sri, Zhengqing, Haru, Alessandro, Rafik, Stefan, Amanj for the friendly relations, mutual helping out and wonderful sense of humor, which were never in a short supply at our room.

Present and former colleagues and fellow students at the GV from all over the world for being always helpful, open for discussion and making my stay at the lab such a pleasant learning experience at many different levels.

My Slovak friends here in Sweden - namely Milan Chromek for enjoyable tennis matches, interesting discussions and mutual lunches. Igor, Jarka and Alicka Dohňanskí for their wonderful hospitality, which helped me to feel home away from my homeland. Dušan Daučík, Kornelia Johansson and Milan Preiberg for their friendship, unworldly help and support.

The ”Nockebynians” for a wonderful athmosphere of friendship and understanding in spite of our diverse backgrounds, that enabled us to stay in contact throughout the years: Max and Ilaria, Pablo, Vasilis, Alexis, Dušan, Michelle and Perry, Annalisa, Stefania, Sabrina, Sandra and Michailo, Manoush, Yuri and the others.

KI tennis friends – Jill, Vino, Fiona, Milan, Dennis, Martin, Konstantin, Darlington and the others for all those great, relaxing matches and good laughs.

All my ”Swedish” friends, namely Dorotka, Agnieszka, Janka and Brano, Janka E., Majka, Claes, John, Tibor, Martin, Hans and the others.

My clinical colleagues and personnel at the ENT department of Södertälje sjukhus for their kind acceptance upon my return to the clinical practice, as well as for all the help, tolerance and understanding during the finalizing stages of my dissertation work.

Na záver chcem zo srdca poďakovať ľuďom mne najbližším - svojim milovaným rodičom za ich nezištnú lásku, obetavú starostlivosť a všestrannú podporu s ktorými som mohol vždy rátať a za ktoré som im neskonale vďačný. Ďakujem tiež mojej sestre Silvií s manželom Jozefom a ich deťmi Katkou a Miškom za všetku pomoc, podporu a krásne, spoločne strávené chvíle.

Thanks also to the ones, I might have forgotten to name here.

This research work was supported by grants from the Swedish Research Council, the Foundation Tysta skolan, the Petrus and Augusta Hedlund Foundation, the European Commision Quality of Life Programme, the Human Frontier Science program, Hörselskadades Riskförbund, the Åke Viberg Foundation, the Tore Nilsson Foundation, the Swedish Society of Medicine and funds from the Karolinska Institutet.

7 REFERENCES

Boutet de Monvel, J., Le Calvez, S. & Ulfendahl, M., 2001. Image restoration for confocal microscopy: Improving the limits of deconvolution, with application to the visualization of the mammalian hearing organ. Biophys. J. 80: 2455-2470.

von Békésy, G., 1960. Experiments in hearing, New York, McGraw-Hill.

Brownell, W.E., Bader, C.R., Bertrand, D. & de Ribaupierre, Y., 1985. Evoked mechanical responses of isolated cochlear outer hair cells. Science 227: 194-6.

Cody, A.R, Russell, I.J., 1988. Acoustically induced hearing loss: Intracellular studies in the guinea pig cochlea. Hearing Res 35: 59-70.

Corey, D., and Hudspeth, A.J., 1979. Ionic basis of the receptor potential in a vertebrate hair cell. Nature 281: 675-677.

Corey, D., García-Añoveros, J., Holt, J.R., Kwan, K.Y., Lin, S.Y., Vollrath, M.A., Amalfitano, A., Cheung, E.L., Derfler, B.H., Duggan, A., Géléoc, G.S., Gray, P.A., Hoffman, M.P., Rehm, H.L., Tamasauskas, D., Zhang, D.S., 2004. TRPA1 is a candidate for the mechanosensitive transduction channel of vertebrate hair cells. Nature 432(7018): 723-30.

Crawford, A.C., Fettiplace, R., 1985. The mechanical properties of ciliary bundles of turtle cochlear hair cells. J. Physiol. 364: 359-79.

Dallos, P., Billone M.C., Durrant, J.D., Wang, C.-Y. & Raynor, S., 1972. Cochlear inner and outer hair cells: Functional differences. Science 177: 356-358.

Dallos, P. 1986. Neurobiology of cochlear inner and outer hair cells: Intracellular recordings. Hearing Res 22: 185 – 198.

Dallos, P., 2008. Cochlear amplification, outer hair cells and prestin. Curr Opin Neurobiol. 18: 370-376.

Engström, B., Borg, E., 1981. Lesions to cochlear inner hair cells induced by noise. Arch Otorhinolaryngol. 230: 279-284.

Engström, B., 1983. Stereocilia of sensory cells in normal and hearing impaired ears. A morphological, physiological and behavioural study. Scand Audiol Suppl. 19: 1-34.

Fettiplace, R., Hackney, C.M., 2006. The sensory and motor roles of auditory hair cells. Nat. Rev. Neurosci. 7(1): 19-29.

Flock, Å., 1965. Transducing mechanisms in the lateral line canal organ receptors. Cold Spring Harb Symp Quant Biol. 30: 133-145.

Flock, Å., Cheung, H.C., 1977. Actin filaments in sensory hairs of inner ear receptor cells. J Cell Biol. 75: 339-345.

Flock, Å., Scarfone, E., Ulfendahl, M., 1998. Vital staining of the intact hearing organ: visualization of cellular structure with confocal microscopy. Neuroscience 83: 215-228.

Flock, Å., Flock, B., Fridberger, A., Scarfone, E., Ulfendahl, M., 1999. Supporting cells contribute to control of hearing sensitivity. J. Neurosci. 19: 4498-4507.

Franke, R., Dancer, A., Khanna, S.M. & Ulfendahl, M., 1992. Intracochlear and extracochlear sound pressure measurements in the temporal bone preparation of the guinea-pig. Acustica 76: 173-182.

Fredelius, L., Johansson, B., Bagger-Sjöbäck, D., Wersäll, J., 1987. Qualitative and quantitative changes in the guinea pig organ of Corti after pure tone acoustic overstimulation. Hearing Res 30: 157-167.

Fredelius, L., 1988. Time sequence of degeneration pattern of the organ of Corti after acoustic overstimulation. A transmission electron microscopy study. Acta Otolaryngol. 106(5-6): 373-385.

Fridberger, A., Flock, Å., Ulfendahl, M., Flock, B., 1998. Acoustic overstimulation increases outer hair cell Ca^{2+} concentrations and causes dynamic contractions of the hearing organ. Proc Natl Acad Sci U.S.A. 95: 7127-7132.

Fridberger, A., Boutet de Monvel, J., Ulfendahl, M., 2002a. Internal shearing within the hearing organ evoked by basilar membrane motion. J. Neurosci. 22: 9850-9857.

Fridberger, A., Zheng, J., Parthasarathi, A., Ren, T. & Nuttall, A., 2002b. Loud sound-induced changes in cochlear mechanics. J Neurophysiol. 88: 2341-8.

Fridberger, A., Boutet de Monvel, J., 2003. Sound-induced differential motion within a hearing organ. Nat Neurosci. 6(5): 446-448.

Fridberger, A., Widengren, J. and Boutet de Monvel, J., 2004. Measuring hearing organ vibration patterns with confocal microscopy and optical flow. Biophys. J. 86: 535-543.

Galambos, R., 1956. Suppresion of auditory nerve activity by stimulation of efferent fibres to cochlea. J Neurophysiol 19: 424-437.

Hamernik, R.P., Turrentine, G., Roberto, M., Salvi, R., Handerson, D., 1984. Anatomical correlates of noise-induced mechanical damage in the cochlea. Hearing Res. 13: 229-247

Hu, X., Evans B.N., Dallos, P., 1999. Direct visualization of organ of Corti kinematics in a hemicochlea. J. Neurophysiol. 82(5); 2798-2807.

Hudspeth, A., J., 1989. How the ear's works work. Nature 341: 397-404.

Hudspeth, A., J., and Corey, D.P., 1977. Sensitivity, polarity and conductance change in the response of vertebrate hair cells to controlled mechanical stimuli. Proc Natl Acad Sci U.S.A. 74: 2407-2411.

Henderson, D., Bielefeld, E.C., Harris, K.C. and Hu, B.H., 2006. The role of oxidative stress in noise-induced hearing loss. Ear Hear. 27: 1-19.

Husbands, J.M., Steinberg, S.A., Kurian, R., Saunders, J.C., 1999. Tip-link integrity on chick tall hair cell stereocilia following intense sound exposure. Hearing Res. 135: 135-45.

Jacob, S., Tomo, I., Fridberger, A., Boutet de Monvel, J. and Ulfendahl, M., 2007. Rapid confocal imaging for measuring sound-induced motion of the hearing organ in the apical region. J. Biomed. Opt. 12(2): 021005.

Kwan, K.Y., Allchorne, A.J., Vollrath, M.A.,Christensen, A.P., Zhang, D.S., Woolf, C.J., Corey, D.P., 2006. TRPA1 contributes to cold, mechanical and chemical nociception but is not essential for hair-cell transduction. Neuron 50(2): 277-89.

Liberman, M.C., Kiang, N.Y., 1978. Acoustic trauma in cats. Cochlear pathology and auditory-nerve activity. Acta Otolaryngol Suppl. 358: 1-63.

Liberman, M.C., Dodds, L.V., 1984. Single-neuron labeling and chronic cochlear pathology. II. Stereocila damage and alterations of spontaneous discharge rates. Hearing Res. 16: 43-53.

Liberman, M.C., Dodds, L.V., 1987. Acute ultrastructural changes in acoustic trauma: serial-section reconstruction of stereocilia and cuticular plates. Hearing Res. 26: 45-64.

Lim, D.J., 1986. Functional structure of the organ of Corti; a review. Hearing Res. 22: 116-146.

Maier, H., Zinn, C., Rothe, A., Tiziani, H., Gummer, A.W.,1997. Development of a narrow water-immersion objective for laserinterferometric and electrophysiological applications in cell biology. J. Neurosci. Methods 77: 31-41.

Merchant, S.N., Ravicz, M.E., Puria, S., Voss, S.E., Whittemore, K.R. Jr., Peake, W.T., Rosowski, J.J., 1997. Analysis of middle ear mechanics and application to diseased and reconstructed ears. Am J Otol. 18: 139-154.

Mulroy, M.J., Whaley, E.A., 1984. Structural changes in auditory hairs during temporary deafness. Scan Electron Microsc. (Pt 2): 831-40.

Nordmann, A.S., Bohne, B.A., Harding, G.V., 2000. Histopathological differences between temporary and permanent threshold shift. Hearing Res. 139: 13-30.

Nowotny, M., Gummer, A.W., 2006. Nanomechanics of the subtectorial space caused by electromechanics of cochlear outer hair cells. Proc Natl Acad Sci USA. 103: 2120-5.

Patuzzi, R., 2002. Non-linear aspects of outer hair cell transduction and the temporary threshold shift after acoustic trauma. Audiol Neurootol. 7: 17-20.

Pawley, J.S., 1995. Handbook of Biological Confocal Microscopy, 2nd ed. Plenum Press, New York.

Puel, J.L., Ruel, J., Gervais d'Aldin, C., & Pujol, R., 1998. Exitotoxicity and repair of cochlear synapses after noise-trauma induced hearing loss. Neuroreport, 9: 2109-14.

Robertson, D., 1983. Functional significance of dendritic swelling after loud sounds in guinea pig cochlea. Hearing Res. 9: 263-78.

Robertson, D., 1982. Effects of acoustic trauma on stereocilia structure and spiral ganglion cells tuning properties in guinea pig cochlea. Hearing Res. 7: 55-74.

Robles, L., Ruggero, M.A., 2001. Mechanics of the mammalian cochlea. Physiol. Rev. 81: 1305-1352.

Rydmarker, S., Nilsson, P., 1987. Effects on the inner and outer hair cells. Acta Otolaryngol Suppl. 441: 25-43.

Saunders, J.C., Dear, S.P., Schneider, M.E., 1985. The anatomical consequences of acoustic injury: A review and tutorial. J. Acoust Soc Am. 78: 833-860.

Saunders, J.C., Cohen, Y.E., Szymko, Y.M., 1991. The structural and functional consequences of acoustic injury in the cochlea and peripheral auditory system: a five years update. J. Acoust Soc Am 90: 136-146.

Smith, C.A., Lowry, O.H., and Wu, M-L., 1954. The electrolytes of the labyrinthine fluids. Laryngoscope 64: 141-153.

Spoendlin, H., 1971. Primary structural changes in the organ of Corti after acoustic overstimulation. Acta Otolaryngol. 71: 166-76.

Spoendlin, H., 1972. Innervation densities of the cochlea. Acta Otolaryngol. 73: 235-248.

Sutinen, P., Zou , J., Hunter, L.L., Toppila, E., Pyykkö, I., 2007. Vibration-induced hearing loss: mechanical and physiological aspects. Otol. Neurotol. 28(2): 171-177.

Thorne, P.R., Gavin, J.B., Herdson, P.B., 1984. A quantitative study of the sequence of topographical changes in the organ of Corti following acoustic trauma. Acta Otolaryngol. 97(l-2): 69-81.

Thorne, P.R., Gavin, J.B., 1985. Changing relationship between structure and function in the cochlea during recovery from intense sound exposure. Ann Otol Rhino Laryngol. 94(1 Pt 1): 81-86.

Thorne, P.R., Duncan, C.E., Gavin, J.B., 1986. The pathogenesis of stereocilia abnormalities in acoustic trauma. Hearing Res. 21: 41-49.

Tsuprun, V., Schachern, P.A., Cureoglu, S., Papparela, M., 2003. Structure of the stereocilia side links and morphology of auditory hair bundle in relation to noise exposure in the chinchilla. J Neurocytol. 32: 1117-28.

Ulfendahl, M., Khanna, S.M., Flock, Å. 1996a. The vibration pattern of the hearing organ in the waltzing guinea pig measured using laser heterodyne interferometry. Neuroscience 72: 199-212.

Ulfendahl, M., Khanna, S.M., Fridberger, A., Flock, Å., Flock, B. & Jäger, W., 1996b. Mechanical response characteristics of the hearing organ in the low-frequency regions of the cochlea. J. Neurophysiol. 76: 3850-3862.

Ulfendahl, M., 1997. Mechanical responses of the mammalian cochlea. Prog. Neurobiol. 53: 331-380.

Ulfendahl, M., Flock, Å. & Khanna, S.M. 1989. A temporal bone preparation for the study of cochlear micromechanics at the cellular level. Hearing Res 40: 55-64.

Ulfendahl, M., Scarfone, E., Flock, Å., Le Calvez, S., Conradi, P., 2000. Perilymphatic fluid compartments and intercellular spaces of the inner ear and organ of Corti. Neuroimage 12: 307-313.

Ulfendahl, M., Boutet de Monvel, J., Le Calvez, S., 2002. Exploring the living cochlea using confocal microscopy. Audiol. Neuro/otol. 7: 27-30.

Wang, Y., Hirose, K., and Liberman, M.C., 2002. Dynamics of noise-induced cellular injury and repair in the mouse cochlea. J. Assoc Res Otolaryngol. 3: 248-268.

Willemin, J.-F., Khanna, S.M. & Dändliker, R., 1989. Heterodyne interferometer for cellular vibration measurement Acta Otolaryngol Suppl. 467: 35-42.

Zhao, Y., Yamoah, E.N., Gillespie, P.G., 1996. Regeneration of broken tip links and restoration of mechanical transduction in hair cells. Proc Natl Acad Sci. U.S.A. 93: 15496-74.

Zheng, J., Shen, W., He, D.Z., Long, K.B., Madison, L.D. & Dallos, P., 2000. Prestin is the motor protein of cochlear outer hair cells. Nature 405: 149-55.

Zou, J., Bretlau, P., Pyykkö, I., Starck, J., Toppila, E., 2001, Sensorineural hearing loss after vibration: an animal model for evaluating prevention and treatment of inner ear hearing loss. Acta Otolaryngol. 121(2): 143-8.